Characterizing quantitative measurements of force and displacement with optical tweezers on the NanoTracker™

Introduction

Optical tweezers are a non-invasive technique to trap, manipulate and track particles. The physical principle behind optical tweezers is the radiation-pressure mediated attraction of refractile particles towards the centre of a focused laser beam, where it becomes trapped. After the emergence of optical tweezers, the technique has been used to manipulate and sort objects. As cells and organelles can be trapped directly thanks to their optical density, they were literally in the 'focus' of the first optical tweezers applications. With the evolution of high-resolution detection techniques, optical tweezers have started to be used extensively to directly and accurately measure the minute forces (in the order of fractions of picoNewtons) involved in molecular interactions. Most often, the biomolecules of interest are not trapped themselves directly, but manipulated through functionalized microspheres.

The trap as such acts as a harmonic potential, in which the restoring force on the particle is proportional to its displacement from the trap center. When working with isotropic probes like polystyrene or silica beads, the trap can be accurately calibrated to perform high-resolution force and displacement measurements. The relative position of the particle can be measured by imaging the probe particle onto a camera or position-sensing detector. This technique is useful for immobile traps. For a mobile trap, so-called back-focal-plane interferometry is the technique of choice [1, 2]. Here, the interference pattern of the laser light with the scattered light is detected, culminating in a high-resolution read-out of the particle displacement from the trap center, independent of the trap position in the sample plane. This form of detection therefore renders the realignment of the detectors during the manipulation of the trap unnecessary. The S-shaped detector response for a microsphere displaced by a distance δ from the trap center is plotted in fig. 1 for a sphere diameter of 0.5 µm. As seen in the figure, for small displacements ($|\delta|$<150 nm), the response is linear (dashed line and shaded area).

For this sort of quantitative force and displacement measurements, the detector sensitivity and the stiffness of the trap of the actual experimental setup used need to be characterized. Both the stiffness of the trap and the escape force (maximal force applicable to the trapped bead) depend on several parameters, most notably the particle size and the laser power. This makes the particle size one of the most important parameters to choose during the design of an experiment.

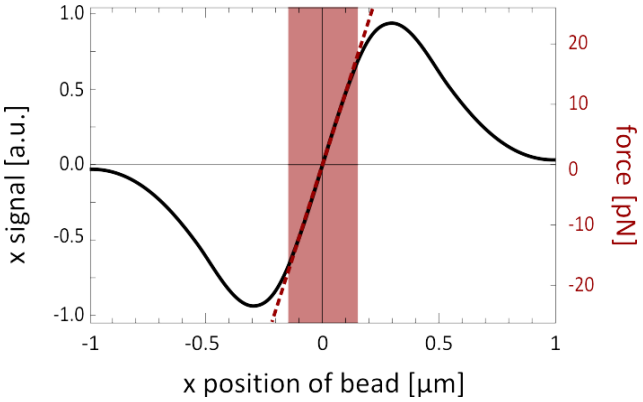

Fig. 1: S-shaped detector response for a sphere *d*=0.5 µm. The central linear range (shaded) can be calibrated to displacements or forces as indicated.

In this report, we present calibration data of diverse microspheres under various conditions characteristic for the JPK NanoTracker™ optical tweezers platform. The report demonstrates the impact of the following experimental variables onto force and spatial resolution: bead material, laser power, trapping objective and measurement bandwidth.

Experimental setup

For the experiments in this report, we have used the new JPK quantitative optical tweezers platform, the NanoTracker™, mounted on a Zeiss Axio Observer inverted optical microscope (see figure 2). This compact system consists of a laser steering unit comprising two individually

and 3-dimensionally steerable beam paths, optimized for stability. The customized microscope body features both a long-distance motorized XY translation stage and a closed-loop 100x100x100 μm^3 piezo stage.

On top of the sample stage, a dual-axis XYZ detection unit is positioned to independently detect 3-dimensional forces and displacements for the two traps. This detection is based on the interferometry scheme mentioned in the introduction. To increase sensitivity, separate detectors are implemented for lateral (XY) and axial (Z) detection. Moreover, axial detection is further enhanced by the application of a pinhole to reject high-angle rays [3].

The NanoTracker™ graphical user interface (GUI) offers full control of the hardware and a convenient automation of measurements. The software includes the online high-bandwidth power spectrum calibration for all channels, which enables performing measurements and recording data in the units of choice. The calibration procedure relies on the latest Lorentzian curve fitting routines available in the literature [4].

Fig. 2: The JPK NanoTracker™ optical tweezers platform, including the laser steering unit, the optical microscope and the detection unit.

Calibration procedure

Due to the dependence on various instrumental and experimental parameters, it is hard or even impossible to theoretically calculate the force exerted by the trapping laser beam on the trapped particle. However, it is possible to use the trapping light that is scattered by the object to get an accurate measure for external forces (i.e., other than the trapping force) acting upon the trapped object. These external forces tend to push or pull the object from the center of the trap. The refractive object, in turn, acts like a little lens and refracts the rays passing through it. The far-field interference of the laser light with the scattered light from the trapped particle, collimated by a detection lens, can be used to get a sensitive measure for the displacements of the trapped particle from the focus. If the trap steering scheme is well-chosen, the intensity distribution in the back focal plane (BFP) of the condenser lens does not change when moving the optical trap around in the sample; the distribution is only affected by motion of the trapped object with respect to the laser focus. When imaging the light distribution in the BFP onto a position-sensitive detector, such as a quadrant photodiode (QPD: a light-sensitive diode which is divided into four equal segments), displacements of the particle in the trap can be measured. Similarly, the total light intensity arriving on the detector yields a measure for the axial particle displacement. This scheme for sensitive 3D displacement detection of a trapped object or the external forces acting on them is known as the aforementioned back-focal-plane interferometry [1, 2].

If a force of known magnitude and direction is applied to the trapped microsphere and one records the corresponding response of the QPD signals, one can calibrate the signals to physically relevant units of either displacement or force. For instance, one can move the sample chamber in which the trapped microsphere is suspended with constant velocity with respect to the position of the trap. The microsphere will be pulled out of the trap along with the sample motion by the viscous drag of the fluid on the microsphere: for a fluid of viscosity η flowing with velocity v along a microsphere of diameter d, the force on the microsphere is $F=3\pi\eta dv=\gamma v$, where γ is the drag coefficient.

Another, more accurate calibration procedure is to make

use of the Brownian motion of the particle. The expected power spectrum of the diffusive Brownian motion exerted by a particle in a viscous liquid and held by a trap of stiffness κ has a Lorentzian shape:

$$S(f) = \frac{k_B T}{\gamma \pi^2 (f_c^2 + f^2)}$$

with $f_c = \kappa / 2\pi\gamma$ the characteristic roll-off or corner frequency of the trap. When the viscosity γ of the medium and the diameter of the particle are known, the stiffness of the trap κ can be derived from the corner frequency, yielding the conversion factor from displacements to forces. Together with the detector sensitivity (in m/V), which is calculated by comparing the measured power spectrum in V²/Hz with the expected one in nm²/Hz, the detector signals can be calibrated either into nanometer displacements within the trap or picoNewton forces. This calibration can be done independently for the two lateral directions (*x*,*y*) and the axial direction (*z*).

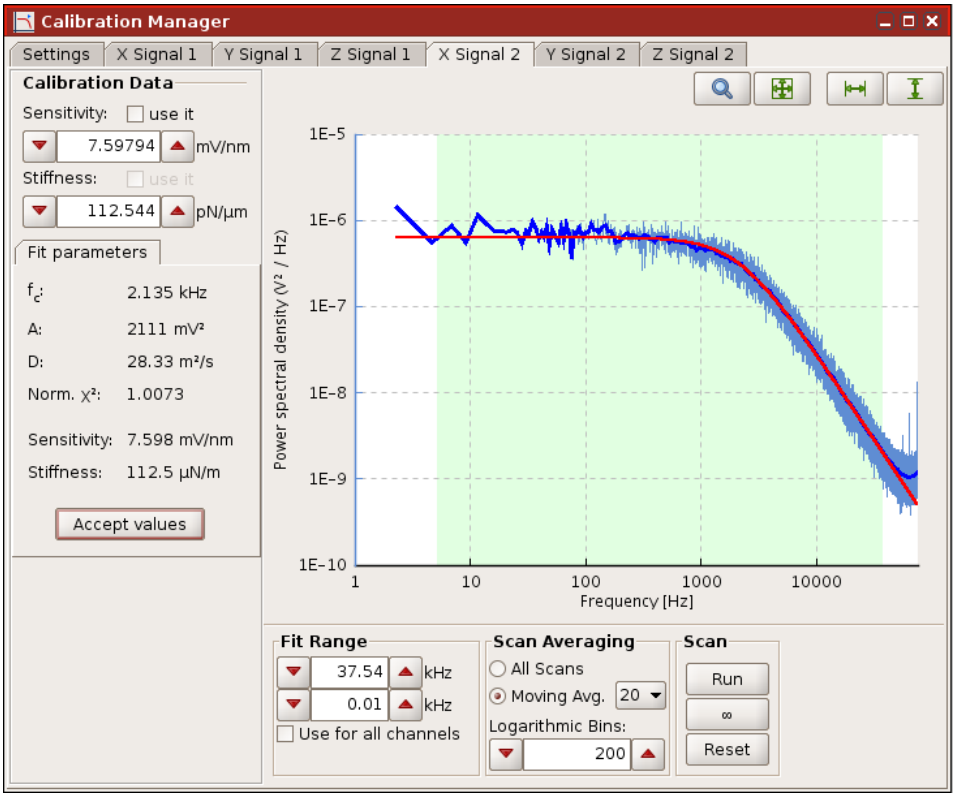

Fig. 3: Screenshot of the NanoTracker™ software, showing the online calibration manager. The program records the thermal noise data originating from the particle's movement inside the trap imaged onto a quadrant photodiode (QPD) (trace in light blue, binned data in dark blue). The fit of a Lorentzian curve (red) to the data yields the sensitivity of the detection and the stiffness κ of the trap. The signal can be calibrated separately for two traps in all directions.

Sensitivity and trap stiffness for different particle sizes and materials

The optical force exerted onto a spherical particle inside a trap depends on the magnitude of refraction of the laser light on the particle surface. Accordingly, at a given laser power, the particle diameter and the difference between the refractive indices of the particle and the surrounding medium have a strong influence on trap stiffness.

As for particle size, there is a range in which particularly high trapping stiffnesses can be generated. This is the case for particle size near the wavelength of the trapping laser [5,

6]. The impact of the refractive index mismatch between the bead and the surrounding liquid on the absolute strengths of trapping can be experienced when trapping materials of different refractive index. The higher the difference in refractive index between particle and surrounding fluid, the larger the force exerted. Hence, polystyrene particles (n = 1.59) experience higher trapping forces than do silica particles (n = 1.43-1.46) in aqueous buffers (n ≥ 1.333).

Here, we present measurements reflecting these relations. Using the NanoTracker™ setup, we have measured both trap stiffness and detection sensitivity for differently sized beads made of polystyrene and silica. The laser intensity was kept constant at 100 mW, measured just behind the detection objective. The results for beads ranging from 50 to 4260 nm in diameter are listed in tables 1 and 2 for polystyrene and silica beads, respectively. For a graphical comparison, the results are plotted in figures 4A and B. In fig. 4A, it can be clearly seen that the stiffness increases steeply in the range from 50 to 1000 nm for both polystyrene and silica particles. For beads larger than 1000 nm, the sensitivity drops again with increasing bead size. As expected, both the trapping strength and the sensitivity are significantly higher for polystyrene particles. The same relationship holds true for the sensitivity of the detection: the detection sensitivity is optimal in the range of 1000 nm (fig. 4B).

bead diameter [nm]	*stiffness [pN/µm]*	*sensitivity [V/µm]*
100	2.06	0.10
200	10.0	0.55
800	220	21.4
1000	355	25.4
4260	140	6.52

Table 1: Lateral trap stiffness and sensitivity of polystyrene beads at a laser intensity of 100 mW.

bead diameter [nm]	*stiffness [pN/µm]*	*sensitivity [V/µm]*
350	37.1	2.65
500	57.8	3.68
1000	211	9.68
2560	159	5.30

Table 2: Lateral trap stiffness and sensitivity of silica beads at a laser intensity of 100 mW.

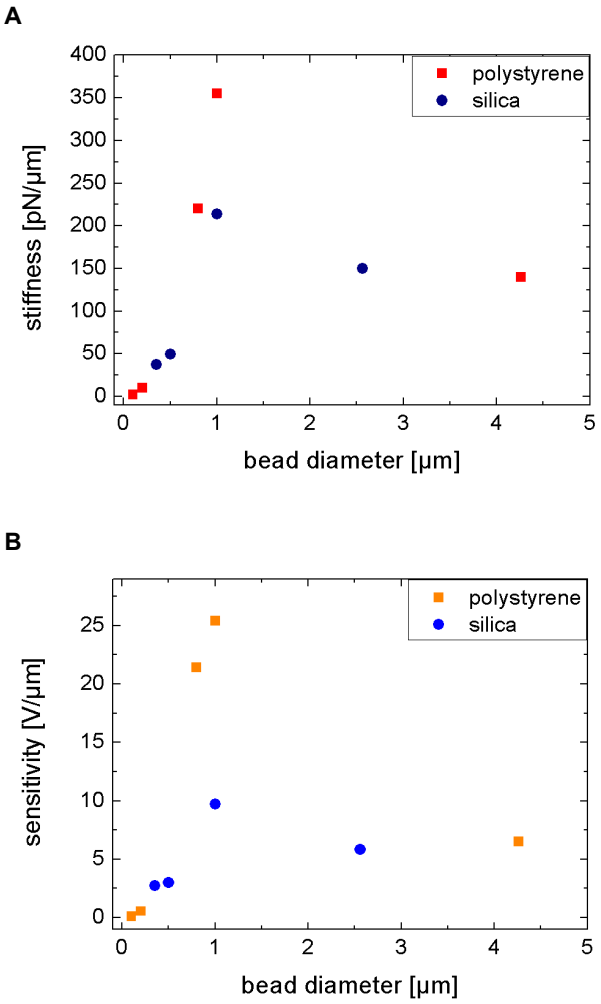

Fig. 4: Dependence of lateral trap stiffness (A) and detection sensitivity (B) on the bead diameter at a laser intensity of 100 mW, measured at the exit from the detection objective. Data for silica and polystyrene beads are plotted.

At this point, it is important to mention that the trap stiffness for a particular bead is not directly correlated to the maximum force applicable to that bead. The escape force of a particle from a trap actually increases steadily with increasing bead size. Accordingly, the particle should be chosen as large as possible for pulling experiments with a maximal escape force, being in the micrometer range (2-5 µm).

It is also possible to trap particles much smaller than the optimal size (down to ~30 nm), which is particularly interesting for tracking experiments, where high forces are typically not required. Choosing the right bead size and type for the measurement is thus strongly application-dependent: it influences the applicable range of forces in the experiment, time scales, sensitivity etc. and therefore determines the design of the experiment.

Sensitivity and trap stiffness at varying laser power

The ability to tune the laser power offers the possibility to vary the stiffness of the trap and the escape force of the bead in the course of the experiment. This instrument feature renders experiments with optical tweezers flexible as to the force range exerted onto a bead. It can be easily switched between two experiment modes: a manipulating trap with a high stiffness and a “soft” trap exerting little influence on the trapped particle, allowing tracking of relatively unhindered motion.

The data of the trap stiffness of a 1 µm bead as a function of laser power show a clear linear dependency (fig. 5), as expected. The detection sensitivity, on the other hand, shows a hyperbolic behavior: at low laser power, the sensitivity increases steeply with increasing power, reaching a plateau at 40 mW in our case. Because of this non-linear behavior, it is crucial to recalibrate the setup when changing the laser power in order to measure correct displacement and force data. The NanoTracker™ comes with selectable attenuation filters in front of the detection, to enhance the dynamic range of the instrument’s detection unit.

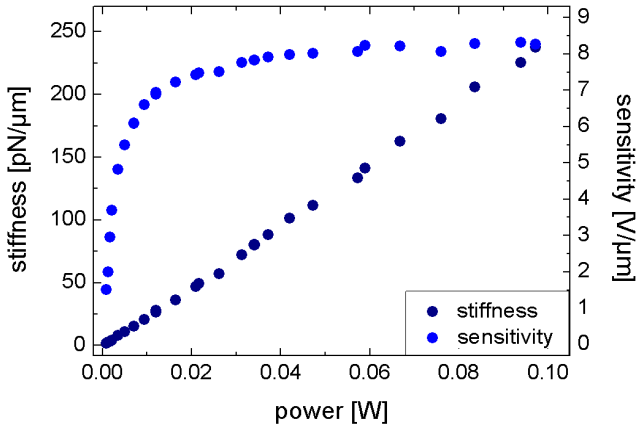

Fig. 5: Lateral trap stiffness and sensitivity of 1 µm silica beads as a function of laser power. Laser power was measured at the exit of the detection objective. Sensitivity was measured with the same attenuation filter in front of the detection unit, to allow comparison.

Sensitivity and trap stiffness at increasing distance to the surface

The trapping objective is a crucial part of the setup, essentially forming the trap. In order to achieve a highly focused laser trap, the Gaussian-shaped laser beam should be coupled into the objective by overfilling it by about 20-50% [7]. Importantly, the objective should be corrected for spherical aberrations and its numerical aperture should be as high as possible, guaranteeing a maximal focusing of the laser beam. Both water and oil immersion objectives are suitable for these purposes, but have their own characteristics that need to be considered. Higher numerical apertures and thus higher trap stiffnesses can be achieved with oil immersion objectives, and are thus to be opted for when high forces are to be generated. Their drawback is that their major application area is experiments on the glass surface or in cells, i.e. in media with refractive indices close to those of oil. When working in water,

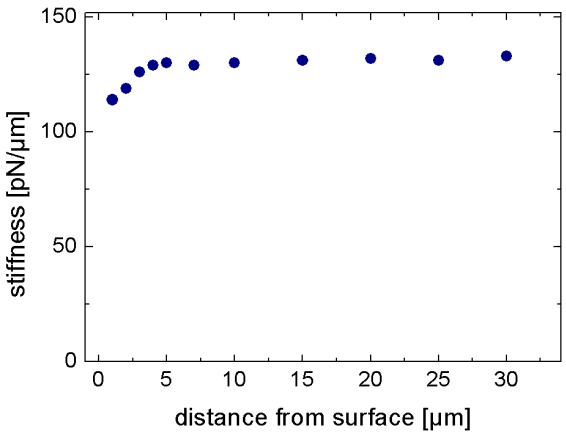

Fig. 6: Lateral trap stiffness of 1 µm silica bead as a function of distance from the glass surface.

spherical aberrations lead to a deterioration of the trap focus that increases with the trap-surface distance [8]. These aberrations can be largely prevented by use of water immersion objectives. The quality of the trap stiffness is constant at increasing distance to the glass surface (see fig. 6). Only at very small distances to the surface, the stiffness appears to reduce because of a higher viscous drag. Generally speaking, the spherical aberrations with water immersion objectives are negligible.

Optimizing measurement conditions

Microscopic objects in a viscous medium undergo Brownian motion. If the particles are also exposed to a harmonic potential – as is the case in an optical trap – the Brownian motion will be confined to a specific volume, limiting the diffusive behavior. This predictable behavior is used for the calibration of the trap, as described before. Furthermore, the measurement of thermal fluctuations of a particle provides information on the particle's interaction with its local environment. Any obstacle will have a pronounced influence on its displacement. Quantitatively, these changes can be tracked by evaluating the fluctuation range of the movement, the shift of the particle's mean position or by looking at the autocorrelation time. The values give quantitative information on local changes in viscosity or particle binding.

The limiting effect of this same Brownian motion comes up when performing force spectroscopy or tracking experiments with optical tweezers. The particle's movement introduces noise into the measurements, fundamentally limiting the spatial, temporal and/or the force resolution of the measurements. Fortunately, these effects can be calculated and the experimental parameters can be tuned to reduce these effects as long as the given experiment permits it. Parameters like the bead size, measurement bandwidth (i.e., sample rate) and stiffness can be optimized to decrease the noise of the probe, which is defined as follows:

$$\delta x = \frac{\sqrt{4k_B TB\gamma}}{\kappa}$$

According to this equation, spatial resolution can be improved by decreasing the bandwidth *B* and the viscous drag γ, which itself is proportional to the viscosity of the medium and the diameter of the object. The stiffness κ of the system has the greatest impact on resolution, which includes both the intrinsic stiffness of the probe and the stiffness of the molecule attached to the probe. In the case of optical tweezers, the probe stiffness is determined not only by the trap stiffness for a particular bead, but also by the stiffness of the tether linking molecule and probe. This tether stiffness can often be tuned in practice, since it depends nonlinearly on the (pre)tension on the linkage.

The impact of changes in trap stiffness and bandwidth on

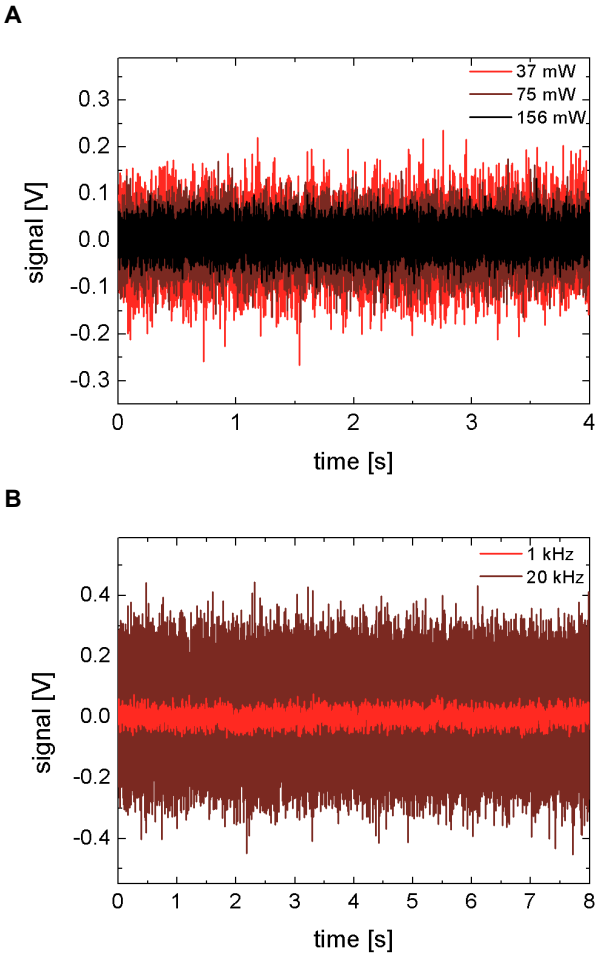

Fig. 7: Influence of laser intensity and detection rate on the thermal noise of a 1 µm bead on the x-axis. (A) Noise reduction due to increasing laser intensity and thus higher stiffness. The data were recorded at 5 kHz. (B) Noise reduction due to lower sampling rate. The data were recorded at a laser intensity of 75 mW at the exit of the detection objective.

the noise are shown in figure 7A and B, respectively. With increasing laser intensity and thus increasing trap stiffness, the noise of the detection signal caused by particle motion decreases (fig. 7A). The movement of the trapped bead is obviously confined to a smaller volume. Due to the high speed of Brownian motion, resolution can also be strongly increased by low-pass filtering or averaging the signal. The data in fig. 7A are recorded at 5 kHz, in fig. 7B the impact of reducing the bandwidth from 20 kHz to 1 kHz is presented: filtering the data significantly reduces the intrinsic noise.

Conclusions & Outlook

With the JPK NanoTracker™, displacement and force measurements become easily accessible without the hassle of time-consuming in-house instrumentation development and system maintenance. Setup considerations as separate detection in xy and z, back-focal plane detection and an ultra-stable laser steering box add up to these high quality experimental data. Additional user comfort is generated amongst others by a tunable laser, fully motorized setup and automated calibration. The measurements presented in this technical report show that the platform delivers trap quality that lives up to the standards of home-built optical tweezers systems.

Literature

[1] Gittes, F. & Schmidt, C. (1998), 'Interference model for back-focal-plane displacement detection in optical tweezers', *Optics Letters* **23**(1), 7-9.

[2] Pralle, A., Prummer, M., Florin, E., Stelzer, E. & Hörber, J. (1999), 'Three-dimensional high-resolution particle tracking for optical tweezers by forward scattered light', *Microsc Res Techniq* **44**(5), 378-386.

[3] Dreyer, J, Berg-Sørensen, K, Oddershede, L. (2004), 'Improved Axial Position Detection in Optical Tweezers Measurements', *Applied Optics* **43,** 1991-1995.

[4] Berg-Sorensen, K. & Flyvbjerg, H. (2004), 'Power spectrum analysis for optical tweezers', *Rev. Sci. Instr.* **75**, 594-612.

[5] Simmons, RM; Finer, JT; Chu, S and Spudich, JA (1996), 'Quantitative Measurements of Force and Displacement Using an Optical Trap', *Biophys J* **77**, 1813-1822.

[6] Rohrbach, A (2005), 'Stiffness of Optical Traps: Quantitative Agreement between Experiment and Electromagnetic Theory', *Phys Rev Letters* **95**(16), 168102(1-4).

[7] Kim, H; Joo, I; Song, S; Kim, P; Im, K, and Oh, C (2003), 'Dependence of the Optical Trapping Efficiency on the Ratio of the Beam Radius-to-the Aperture Radius', *J Korean Phys Society* **53**(3), 348-351.

[8] Vermeulen, KC; Wuite, GJL, Stienen, GJM and Schmidt, CF (2006), 'Optical trap stiffness in the presence and absence of spherical aberrations', *Applied Optics* **45**(8), 1812-1819.

[9] Neuman, K. C. & Nagy, A. (2008), 'Single-molecule force spectroscopy: optical tweezers, magnetic tweezers and atomic force microscopy.', *Nat Methods* **5**(6), 491-505.